

Optical Engineering

OpticalEngineering.SPIEDigitalLibrary.org

Obliquely incident ion beam figuring

Lin Zhou
Yifan Dai
Xuhui Xie
Shengyi Li

Obliquely incident ion beam figuring

Lin Zhou,^{a,b,*} Yifan Dai,^{a,b} Xuhui Xie,^{a,b} and Shengyi Li^{a,b}

^aNational University of Defense Technology, College of Mechatronic Engineering and Automation, 109 Deya Road, Changsha 410073, China

^bHu'nan Key Laboratory of Ultra-precision Machining Technology, 109 Deya Road, Changsha 410073, China

Abstract. A new ion beam figuring (IBF) technique, obliquely incident IBF (OI-IBF), is proposed. In OI-IBF, the ion beam bombards the optical surface obliquely with an invariable incident angle instead of perpendicularly as in the normal IBF. Due to the higher removal rate in oblique incidence, the process time in OI-IBF can be significantly shortened. The removal rates at different incident angles were first tested, and then a test mirror was processed by OI-IBF. Comparison shows that in the OI-IBF technique with a 30 deg incident angle, the process time was reduced by 56.8%, while keeping the same figure correcting ability. The experimental results indicate that the OI-IBF technique is feasible and effective to improve the surface correction process efficiency. © The Authors. Published by SPIE under a Creative Commons Attribution 3.0 Unported License. Distribution or reproduction of this work in whole or in part requires full attribution of the original publication, including its DOI. [DOI: 10.1117/1.OE.54.10.105101]

Keywords: optical fabrication; ion beam figuring; polishing.

Paper 150886 received Jun. 30, 2015; accepted for publication Sep. 14, 2015; published online Oct. 7, 2015.

1 Introduction

Ion beam figuring (IBF) is a highly deterministic process to fabricate high-precision optics.¹⁻⁵ IBF applies the physical sputtering effect to remove materials from optical surfaces, using an ion beam to bombard the optics. In this process, the surface error materials can be sputtered off by controlling the dwell times of the ion beam at different locations on the optical surface. Thus, the surface error figure can be corrected. Due to its unique way of removing materials by physical sputtering, IBF has many good features, e.g., highly deterministic, high precision, fully electrical control, no load force, no surface and subsurface damage, no edge effect, etc. These features make IBF an advantageous method by which to produce high-precision optics. However, the local heating resulting from the beam bombardment may be a problem to some substrates that are sensitive to thermal shock, and IBF may change surface microroughness.²

In a normal IBF process, the ion beam bombards the optical surface in normal incidence during the whole process. However, the removal rate under an oblique incidence condition is greater than that of the normal incidence.⁶ Therefore, if we perform the IBF process with an oblique incidence angle instead of the normal incidence, the material removal rate can be increased, and the processing time can be shortened.

Although oblique incidence by ion beam has been applied in some studies to investigate the evolution of the surface roughness under ion beam bombardment,⁷ up until now, there has been no dedicated study that investigates correcting the surface error using an oblique ion beam where the incident angle is kept invariable in the whole process.

In this paper, we propose a new IBF processing technique, obliquely incident IBF (OI-IBF). The removal rates at different incident angles were first tested, and then OI-IBF processes were demonstrated with 30 deg incident angles.

2 Method Description

The schematic diagram of the OI-IBF technique is shown in Fig. 1, where Fig. 1(a) shows the normal IBF technique, and Fig. 1(b) shows the OI-IBF technique which keeps the ion beam bombarding the optical surface at the same oblique incidence angle θ during the process.

In OI-IBF, due to the change of the attitude of the ion beam from the normal IBF, the parameters, including the positions and angles, used to control the motion of the ion source should be recalculated. Suppose the motion parameters, which are used to drive the five axes X , Y , Z , A , and B to control the positions and angles of the ion source in the normal IBF, are calculated out as $(x_0, y_0, z_0, \alpha_0, \beta_0)$.⁸ To process a plane sample, we get $\alpha_0 = \beta_0 = z_0 \equiv 0$. When applying the OI-IBF technique, in order to keep the ion beam with an invariant incident angle θ from the optical surface [suppose this angle is achieved by tilting axis B , please refer to Fig. 1(b) for the OI-IBF geometry setup], the new motion parameters (x, y, z, α, β) can be calculated using

$$\begin{cases} x = x_0 - l \sin \theta, & y = y_0, & z = l(1 - \cos \theta), \\ \alpha = 0, & \beta = \theta \end{cases}, \quad (1)$$

where l is the processing target distance.

3 Experiments and Results

3.1 Test on Removal Rates for Different Incident Angles

Experiments were carried out on a self-developed IBF plant with Ar^+ ions.⁹ The main vacuum chamber of the plant has a diameter of ~ 1.5 m and a height of 1.5 m, with four molecular pumps FF-200/1300 from KYKY Technology Co. to pump. The ion source used in our IBF plant is a 5 cm dc ion source of the hollow cathode type from Veeco Instruments Inc. The ion source is mounted on a self-developed five-axis motion platform which has three position axes

*Address all correspondence to: Lin Zhou, E-mail: zhoulin9013@gmail.com

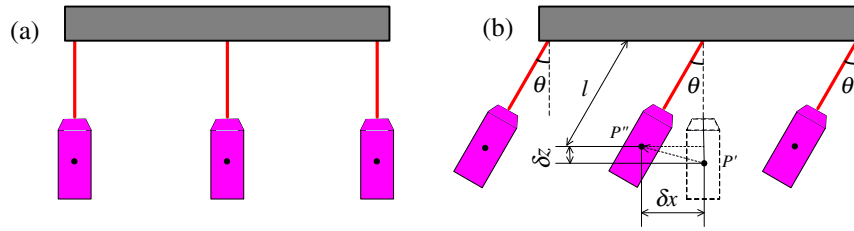


Fig. 1 Schematic diagram of obliquely incident ion beam figuring (OI-IBF): (a) normal IBF technique (ion beam in normal incidence from the optical surface) and (b) OI-IBF technique (ion beam in oblique incidence angle θ from the optical surface).

(XYZ) plus two orientation axes (AB). The XYZ travel is more than $650 \times 650 \times 200 \text{ mm}^3$, and the AB rotation range is -30 to 30 deg. To reduce the time consumed to replace the workpiece in the big vacuum chamber, a small vacuum chamber of about $500 \times 400 \times 600 \text{ mm}^3$ ($W \times H \times D$) is connected to the main chamber via a gate valve. When the gate valve is open, the workpiece can be transported to the big chamber for IBF processing and back to the small chamber after processing automatically. The small chamber is pumped by a molecular pump FF-200/1300, and the pump-down time is <15 min. To achieve a small ion beam, a diaphragm with a hole is mounted on the ion source, which is placed on a position 150 mm away from the ion source grid. The diaphragm can be changed. Therefore, ion beams with different sizes can be achieved. In our experiments, the aperture of the diaphragm is 5 mm, the ion energy is set to 800 eV, and the beam current is set to 25 mA.

First of all, the material removal rates at different incident angles in IBF process should be obtained. To do this, the same ion beam was used to bombard different points in one experiment on a sample with the same bombardment times, but with different incident angles. After the experiment, we can get different etched footprints. With these footprints, the removal rates including peak removal rate (PRR) and volume removal rate (VRR) can be extracted. The sample used in this test is a 100-mm-diameter plane Zerodur substrate. We tested seven different incident angles from 0 to 30 deg. All the resulted seven footprints of different incident angles were conducted to bombard on a line with 12 mm interval and 3 min of bombardment time for each point.

The experimental results are shown in Fig. 2(a), where the seven footprints from left to right are the results of different incident angles from 0 to 30 deg (5 deg interval). The profile

line from left to right through the center of the footprints is shown in Fig. 2(b). The experimental results show that the removal rates get higher as the incident angles increase, as indicated by the sputtering theory.⁶ Although the maximum removal rate occurs at a higher incident angle (60 to 80 deg, the specific angle depends on the bombardment condition), most IBF plants cannot tilt to that high incident angle. The maximum angle possible in our IBF plant is 30 deg.

With the resulting removal footprints, which are already shown in Fig. 2, each footprint can be extracted and its PRR and VRR can be calculated. The resulting PRR, VRR, and also relative PRR and relative VRR, are summarized in Table 1. To illustrate the changes of the removal rates on different incident angles, we have also plotted the curves of relative PRRs and relative VRRs in Fig. 3.

If the value of the relative VRR at incident angle θ is Vr , then it means the removal efficiency will be increased by a factor of Vr , and the process time will be shortened by a factor of $1/Vr$. For example, if we perform OI-IBF with a 30 deg incident angle, according to the experimental result (Table 1), the relative VRR value is 1.76. This means that the removal efficiency of the OI-IBF will be improved by a factor of 176%, and the process time will be reduced by a factor of 56.8%.

3.2 Obliquely Incident Ion Beam Figuring Experiments

The test sample to be processed by OI-IBF is a 100-mm-diameter plane Zerodur. Its initial surface error is 27 nm RMS (the error map is shown in Fig. 4). It was processed in the same IBF plant and using the same processing conditions as described previously.

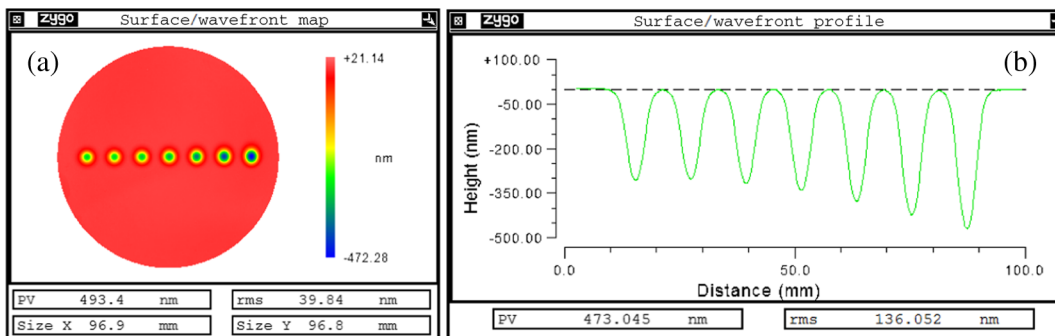
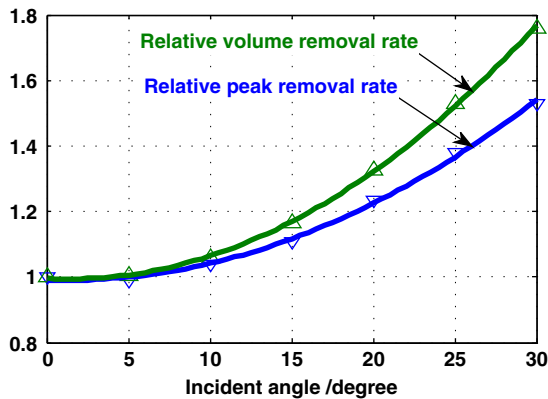
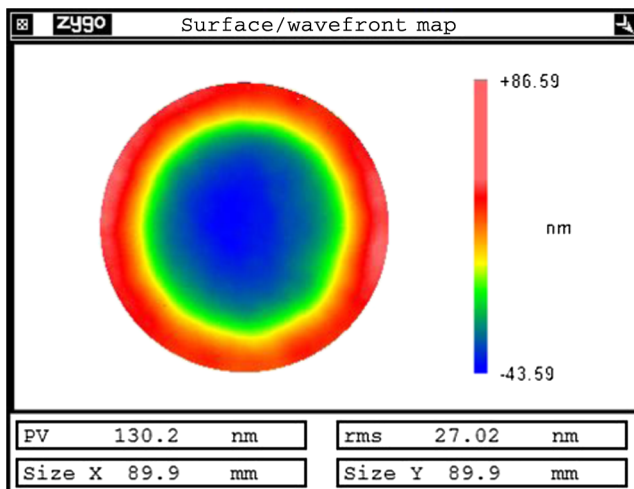


Fig. 2 The experimental result for removal rates at different incident angles: (a) the footprints from 0 to 30 deg (5 deg interval, from left to right) and (b) the profile line through the center of the footprints from left to right.

Table 1 The resulting removal rates at different incident angles from the experiment.

Incident angle	0 deg	5 deg	10 deg	15 deg	20 deg	25 deg	30 deg
Peak removal rate (PRR) (nm/min)	102	101	106	113	126	141	156
Relative PRR	1	0.99	1.04	1.11	1.24	1.38	1.53
Volume removal rate (VRR) ($\times 10^{-3}$ mm ³ /min)	2.05	2.06	2.17	2.39	2.72	3.14	3.61
Relative VRR	1	1.00	1.06	1.17	1.33	1.53	1.76


Fig. 3 The curves showing resulting relative peak removal rate and relative volume removal rate versus incident angles.

Fig. 4 The initial surface error map on the sample before OI-IBF.

For this test optical sample, we calculated the processing times, first with normal IBF and then with OI-IBF. The calculations were done using our self-developed software IBFCAM, which is developed to perform all the calculations involved in an IBF process, including extracting beam removal function, calculating dwell time, predicting residual error, generating G-code used to control the motion of ion source, etc. The calculated results with normal IBF and OI-IBF are shown in Figs. 5 and 6, respectively. Although some of the interface characters are Chinese, we added some English explanations to them and hope it can be easy to read.

In the normal IBF calculation, with the normal removal function [refer to the top-right area of Fig. 5, which is extracted from the leftmost footprint in Fig. 2(a)], the calculated process time is 219.8 min (highlighted with a circle in the bottom-right area of Fig. 5), and the forecasted residual error is 1.09 nm RMS (highlighted with a circle in the bottom-left area of Fig. 5). In the OI-IBF calculation, with a 30 deg incident angle, the corresponding removal function, which is extracted from the rightmost footprint in Fig. 2(a), is shown in the top-right area of Fig. 6. The calculated process time is 125.1 min (highlighted with a circle in the bottom-right area of Fig. 6), and the forecasted residual error is 1.14 nm RMS (highlighted with a circle in the bottom-left area of Fig. 6). Comparing the calculations (Figs. 5 and 6), we can see that although their forecasted residual errors are almost the same, the process time in OI-IBF is significantly reduced by 56.9%. This is highly consistent with the prediction (56.8%) described in Sec. 3.1.

After the first experimental OI-IBF test, the surface error on the test sample was reduced to 5.14 nm RMS [the error map is shown in Fig. 7(a)] from the initial 27 nm RMS (Fig. 4). We, therefore, performed another calculation and again compared the results between the normal IBF and the OI-IBF. The comparison indicates again that although the process time was significantly reduced (from 36.4 min in normal IBF to 20.6 min in OI-IBF, 56.6% reduction), the forecasted residual errors are almost the same (from 0.683 to 0.686 nm RMS). The sample was processed again by OI-IBF, and the final residual surface error is 1.03 nm RMS [the error map is shown in Fig. 7(b)].

4 Discussion

Although we only demonstrated the OI-IBF technique on a plane sample, it can be applied to a general curved optical surface as well. In a general OI-IBF case on curved surfaces, the recalculation of the motion parameters will become a little more complicated. Considering a general case with incident angle vector (ϕ, φ) , it means the ion beam obliquely bombards the surface with angle ϕ (tilting the axis A) and angle φ (tilting the axis B). Therefore, the synthetic incident angle θ is

$$\theta = \cos^{-1}(\cos \phi \cdot \cos \varphi). \quad (2)$$

Then under the incident angle (ϕ, φ) , the new motion parameters in the OI-IBF can be calculated from the knowledge of geometry and kinematics.

$$\alpha = \alpha_0 + \phi, \quad \beta = \beta_0 + \varphi, \quad (3)$$

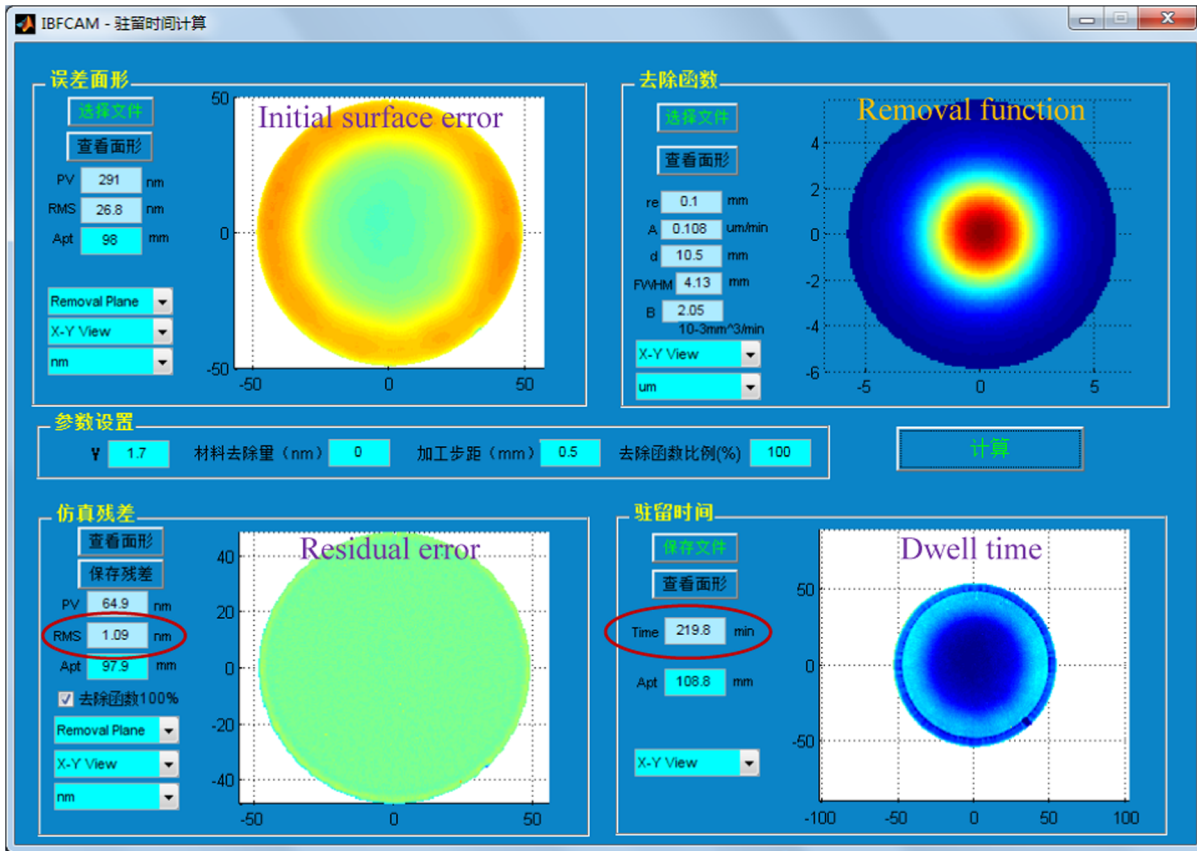


Fig. 5 The calculation results of the normal IBF (screenshot from our IBFCAM software).

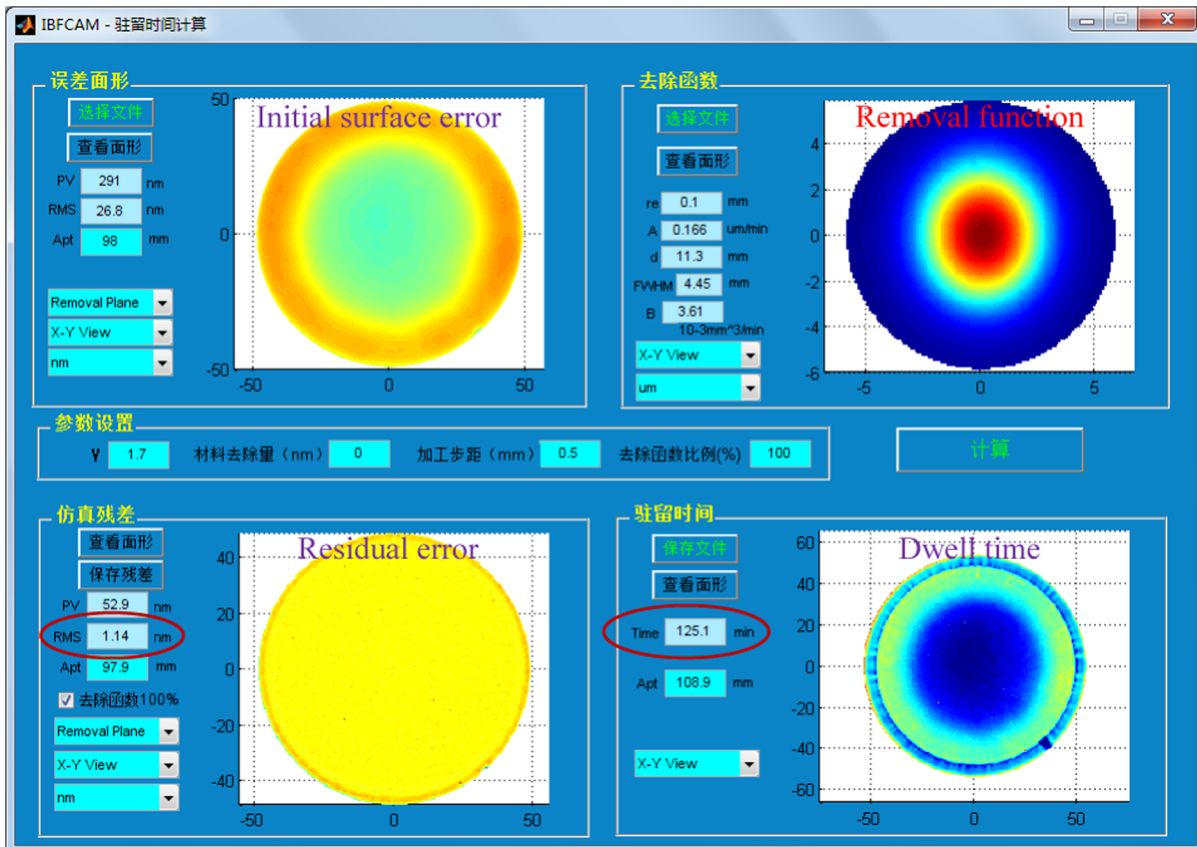


Fig. 6 The calculation results of the OI-IBF (screenshot from our IBFCAM software).

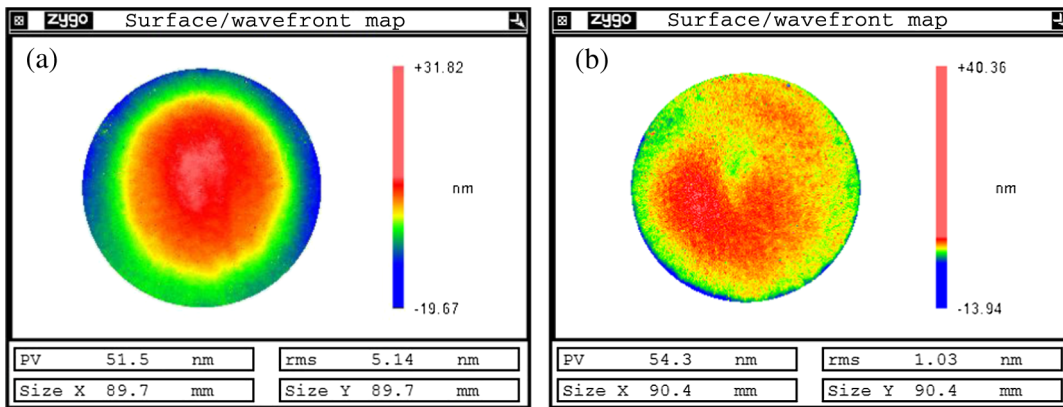


Fig. 7 Experimental surface error maps: (a) the error map after the first OI-IBF process and (b) the error map after the second OI-IBF process.

$$\begin{cases} x = x_0 - l(\sin \beta - \sin \beta_0) \\ y = y_0 + l(\sin \alpha \cos \beta - \sin \alpha_0 \cos \beta_0) \\ z = z_0 - l(\cos \alpha \cos \beta - \cos \alpha_0 \cos \beta_0) \end{cases} \quad (4)$$

In the OI-IBF process, unlike in the normal removal function, the oblique removal function is not rotationally symmetrical. The size of the oblique removal function in the direction parallel to the incident direction will be greater than the size in the perpendicular direction [see Fig. 2(a) and top-right area of Fig. 6]. However, our software uses a general two-dimensional removal function in all calculations. So, any removal functions, whether it is rotationally symmetric or not, can be accepted and calculated as well.

Another effect of the change on the removal function is a larger removal function will result in a weaker figure correcting ability for the surface error.¹⁰ But this effect is very low because the change in the size of the removal function is not significant. The calculations in the Sec. 3.2 have proven this, showing the forecast residual errors are almost the same. This demonstrates that using the OI-IBF technique, we can greatly reduce the process time, while keeping the same figure correcting capability.

Furthermore, some other experiments have shown that normal incidence can increase the surface roughness while oblique incidence can reduce it.¹¹ Therefore, OI-IBF is a promising technique to correct the surface figure error while simultaneously smoothing the surface.

5 Conclusion

We have proposed and experimentally demonstrated that the OI-IBF technique can greatly shorten the processing time and improve processing efficiency, while keeping the same figure correcting capabilities.

Acknowledgments

This work was supported by the National Natural Science Foundation of China (No. 91323302, No. 91023042, and No. 51105370) and the Program for New Century Excellent Talents in University (No. NCET-13-0165).

References

1. S. R. Wilson, D. W. Reicher, and J. R. McNeil, "Surface figuring using neutral ion beams," *Proc. SPIE* **966**, 74–81 (1988)
2. L. N. Allen, "Progress in ion figuring large optics," *Proc. SPIE* **2428**, 237–247 (1994).
3. T. W. Drueding, T. G. Bifano, and S. C. Fawcett, "Contouring algorithm for ion figuring," *Precis. Eng.* **17**(1), 10–21 (1995).
4. A. Schindler et al., "Ion beam finishing technology for high precision optics production," presented at *Optical Fabrication and Testing*, 3 June 2002, Tucson, Arizona, paper OTuB5, Optical Society of America, Washington DC (2002).
5. L. Zhou et al., "Ion beam technology: figuring, adding and smoothing for high-precision optics," presented at *Optical Fabrication and Testing*, 22–26 June 2014, Kohala Coast, Hawaii, paper OM4B.4, Optical Society of America, Washington DC (2014).
6. P. Sigmund, "Theory of sputtering. I. Sputtering yield of amorphous and polycrystalline targets," *Phys. Rev.* **184**, 383 (1969).
7. M. A. Makeev, R. Cuerno, and A. L. Barabási, "Morphology of ion-sputtered surfaces," *Nucl. Instrum. Methods Phys. Res. B* **197**(3–4), 185–227 (2002).
8. L. Zhou et al., "Translation-reduced ion beam figuring," *Opt. Express* **23**, 7094–7100 (2015).
9. W. Liao et al., "Mathematical modeling and application of removal functions during deterministic ion beam figuring of optical surfaces. Part 2: application," *Appl. Opt.* **53**, 4275–4281 (2014).
10. L. Zhou et al., "Frequency-domain analysis of computer-controlled optical surfacing processes," *Sci. China Ser. A* **52**(7), 2016 (2009).
11. Y. Shu et al., "Impact of oblique incidence in ion beam figuring on surface roughness," *Nanotechnol. Precis. Eng.* **10**(4), 365–368 (2012). (in Chinese)

Lin Zhou is an associate professor at the National University of Defense Technology (NUDT). He received his BS, MS, and PhD degrees in mechanical engineering from NUDT in 2001, 2003, and 2008, respectively. He is the author of more than 20 journal papers. He was awarded the New Century Excellent Talents in University in 2013. He visited Brookhaven National Laboratory in United States for one year in 2014. His research interests include optical fabrication and metrology.